Łukasz Łańcucki, Paweł Pasierb*

AGH - University of Science and Technology, Faculty of Materials Science and Ceramics, al. Mickiewicza 30, 30-059 Krakow, Poland
*Corresponding author. E-mail: ppasierb@agh.edu.pl

POLYANILINE/CaTi$_{0.8}$Fe$_{0.2}$O$_3$ COMPOSITES FOR HUMIDITY SENSORS

Polyaniline (PANI) is a conductive polymer material with a huge potential for constructing different electrochemical devices. Different strategies can be used to modify and optimize polymer properties from the point of certain applications, e.g. for the construction of gas sensors. Among those strategies, the formation of composite materials comprising PANI as the base material and ceramic powder material as a modifier is a promising approach. In this work the results concerning the influence of CaTi$_{0.8}$Fe$_{0.2}$O$_3$ (CTFO) powders on some physicochemical properties of polyaniline (PANI) were presented and discussed. The materials were obtained by the polymerization of an aniline solution where CTFO powder, prepared by the sol-gel method was added. The microstructures of the materials were characterized using Scanning Electron Microscopy (SEM), the structure and phase composition was tested by X-ray diffraction (XRD) and Fourier Transform Infrared Spectroscopy (FTIR). The electrical properties of the developed PANI-CTFO composites were determined using Electrochemical Impedance Spectroscopy (EIS). The gas sensing properties of the constructed sensor devices in the presence of water vapor were tested by measurements of DC electrical conductivity changes as a function of water vapor partial pressure. The current--voltage (I-U) characteristics were also used to characterize the influence of CTFO material on PANI electrical properties. It was found that the introduction of CTFO into the PANI host material leads to substantial changes in the material properties comparing to unmodified PANI. The discussion concerning the influence of the used modifiers on the structure, microstructure and electrical and sensing properties of the developed materials and observed correlation is also presented. The mechanism of the observed influence of CTFO on PANI properties is also proposed. The dominating role of the PANI-CTFO interface on the material properties is postulated.

Keywords: polyaniline, nanofiber, composite, iron doped calcium titanate, humidity sensor, conductivity

KOMPOZYTY NA BAZIE POLIANILINY DOMIESZKOWANEJ CaTi$_{0,8}$Fe$_{0,2}$O$_3$ JAKO SENSORY WILGOTNOŚCI

Polianilina (PANI) należy do grupy polimerów przewodzących posiadających ogromny potencjał z punktu widzenia możliwości budowy różnych urządzeń elektrochemicznych. W celu optymalizacji właściwości polimeru pod kątem określonego zastosowania, np. do konstrukcji czujników gazowych, stosuje się różne strategie modyfikacji. Wśród nich obiecującym podejściem jest utworzenie materiałów kompozytowych zawierających jako materiał bazowy PANI i jako modyfikator proszkowy materiał ceramiczny. W pracy przedstawiono wyniki dotyczące wpływu proszków CaTi$_{0,8}$Fe$_{0,2}$O$_3$ (CTFO) na niektóre właściwości fizykochemiczne polianiliny (PANI). Materiały zostały uzyskane przez polimeryzację roztworu aniliny, do których dodano proszku CTFO przygotowanego metodą zol-żel. Mikrostruktura materiałów została określona przy użyciu skaningowej mikroskopii elektronowej (SEM), strukturę i skład fazy zbadano przez dyfrakcję promieniowania X (XRD) i spektroskopii w podczerwieni z transformacją Fouriera (FTIR). Właściwości elektryczne opracowanych kompozytów PANI-CTFO wyznaczono za pomocą pomiarów metodą elektrochemicznej spektroskopii impedancyjnej (EIS). Charakterystyki sensorowe na obecność pary wodnej prototypowych czujników budowanych z otrzymanych materiałów były testowane poprzez pomiar zmian przewodnictwa elektrycznego w funkcji ciśnienia cząstkowego pary wodnej. Wykonano także pomiary charakterystyk prąd-napięcie (I-U), które wykorzystano do dodatkowego scharakteryzowania wpływ materiału CTFO na właściwości elektryczne PANI. Stwierdzono, że wprowadzenie CTFO do materiału bazowego PANI prowadzi do znacznych zmian właściwości materiału w porównaniu do niezmodyfikowanej polianiliny PANI. Przeprowadzono dyskusję dotyczącą wpływu stosowanych modyfikatorów CTFO na strukturę, mikrostrukturę i właściwości elekftryczne badanych materiałów na bazie PANI oraz określono wzajemne korelacje. Uzyskane wyniki wskazują na dominującą rolę granic faz CTFO-PANI na właściwości elektryczne badanych materiałów.

Słowa kluczowe: polianilina, nanowłókna, kompozyt, tytanian wapnia domieszkowany żelazem, sensor wilgotności, przewodnictwo

INTRODUCTION

Humidity sensors have gained great attention for their practical applications in industrial fields, laboratory environment, and our daily life [1]. Presently known analytical techniques usually utilize expensive,

bulky and quite sophisticated equipment. That is why such compact portable solutions allowing rapid local real-time detection as electronic sensors are a promising alternative to time-consuming laboratory techniques. The principle of operation is a quite simple conversion of chemical changes in the sensing layer into an electrically measurable response signal. In this regard, the application of conducting polymers able to reversibly change their characteristics depending on the atmospheric composition is a promising direction in the development of sensing materials [2, 3]. From the wide variety of conducting polymers, polyaniline (PANI) has received great attention due to its environmental stability as well as is its ability to respond to external stimuli by changes in conductivity. Additionally, a variety of PANI nanostructures can be prepared, therefore the development of PANI based materials is almost unlimited [4]. Polyaniline was first synthesized in 1862 [5] and has been extensively studied as a conducting polymer since the 1980s [6, 7]. Depending on the synthesis conditions, it can be obtained in several forms and with different structures. By adjusting the pH of the polymerization process to mildly acidic, it is possible to synthetize PANI in the form of nanofibers and nanotubes [8]. Moreover, doping of conducting polymers with inorganic additives can further improve their abilities [9]. Therefore, the intercalation of conducting polymers, such as polyaniline, polypyrrole and polythiophene, in inorganic hosts has also been a topic of considerable interest. The resulting composite materials obtained through the dispersion of metal oxides and other inorganic powders in the polymer matrix has been widely explored due the wide range of potential applications in diverse areas [10, 11]. Precisely for this reason, the combination of characteristics of the parent constituents into a single material have been researched because ceramics exhibit high dielectric performance and polymers have low costs and can be easily processed [12]. The dopant choice significantly influences the polymer sensitivity to humidity and predetermines its structure, morphology, and conductivity [13]. An improvement in response time, sensitivity, detection limit, stability and durability can usually be achieved by aniline polymerization in the presence of semiconducting metal oxide nanoparticles (e.g. TiO_2, ZnO, SnO_2) [14, 15]. Composites of conducting polymers with numerous types of inorganic oxides have been utilized for humidity sensing. These metal oxides must be physically and chemically stable as confirmed during tests performed at both room and elevated temperatures [16, 17]. The current focus is on the development of polyaniline ceramic sensor composites based on the perovskite family using in-situ polymerization processes. Perovskite materials is a large family of crystalline ceramics which are of practical importance due to their dielectric, piezoelectric, ferroelectric, and mechanical properties. Sensors based on perovskite type oxides have an advantage of high stability. First

and foremost, the family of compounds based on an original perovskite crystal structure shows an enormous variety of structural modifications and variants in their physical and chemical properties. The perovskite structure from $CaTiO_3$ (CTO), is often encountered in solid state inorganic chemistry [18]. Furthermore, doping CTO with iron ions increases its conductivity without affecting the perovskite sensing properties towards water molecules [19]. In this study, firstly, $CaTi_{0.8}Fe_{0.2}O_3$ (CTFO) particles were produced by the sol-gel technique, PANI-CTFO composites were obtained with aniline, and the polymeric matrix was synthesized by the emulsion polymerization method. Their structural characterization was analyzed by XRD, SEM and FT-IR analysis. DC measurements were analyzed to study composite conductivity at temperatures up to 150°C and sensing properties toward water. To the best of our knowledge, this is the first ever attempt made to study these composites as humidity sensors. In this article, we describe our attempt to modify polyaniline by implementing iron substituted calcium titanate, as the addition of such an inorganic dopant is expected to improve polymer stability. The main aim of this work was to investigate how the addition of CTFO to the polyaniline bulk would affect the PANI sensing properties.

EXPERIMENTAL PROCEDURE $CaTi_{0.8}Fe_{0.2}O_3$ SYNTHESIS

Herein, we describe the synthesis of $CaTi_{0.8}Fe_{0.2}O_3$ (CTFO) powders via the sol-gel technique: 0.08 M of $Ti(O\text{-}iPr)_4$ - titanium(IV) isopropoxide (Aldrich, pure p.a.) was mixed with 80 cm^3 anhydrous ethanol and stirred constantly, next a mixed solution of 0.2 M citric acid monohydrate and $3 \cdot 10^{-4}$ M nonionic surfactant - octyl phenol ethoxylate (TX-100, Avantor, pure p.a.) was added, afterward a mixed solution of 0.1 M calcium nitrate (Avantor, pure p.a.) and 0.02 M iron(III) nitrate (Avantor, pure p.a.) was added to the above mixture and the resultant solution was stirred constantly for 30 min. In order to stabilize the solution, 2.5 g of polyvinyl alcohol (mw 720000, Avantor) was added. Finally, the resulting sol was dried at 100°C to form a xerogel and was further dried in air at 200°C for 12 h, then ground to obtain a fine powder. This method gives a Ca/Ti/Fe/Citric acid molar ratio of 10/8/2/20. The powder was then pressed into pellets and heated at a rate of 2°C/min to a temperature of 600°C where it was kept for 10 h [20]. Finally, the obtained powder was finely ground and the fraction of 90÷63 μm was used for composite fabrication.

POLYANILINE SYNTHESIS

Synthesis of all the samples, both PANI and its composites, was carried in a 250 cm^3 two-neck flask.

During both the preparation and polymerization processes, the solution was intensively stirred and bubbled with helium (2.2, Alphagaz) in order to remove residual oxygen that could affect the polymerization process. The final volume of the solutions for all the samples was 150 cm^3. A typical one-step route PANI synthesis procedure by oxidation polymerization is as follows: 0.06 M aniline (Avantor, pure, p.a.) was mixed with 0.5 M acetic acid (Avantor, pure p.a.). The above solution was stirred for 30 min. Aniline polymerization was started at 25°C by adding 0.06 M APS - ammonium peroxydisulfate (Avantor, pure p.a.) that was dissolved in 50 cm^3 of 0.5 M acetic acid, The resultant pH of the final solution was 3.7. The mixture was constantly stirred during polymerization for 120 min. After polymerization, a small amount of 2-propanol (2 cm^3) was added to the flask to terminate the micro-emulsion system. The precipitate dark green powder was vacuum filtered and washed several times with water in order to remove contaminants from the solution. Finally, the resultant precipitate was dried in an oven for 24 hours at 80°C to achieve a constant weight.

SYNTHESIS OF PANI-CaTi$_{0.8}$Fe$_{0.2}$O$_3$ COMPOSITES

PANI composites were obtained via a similar polymerization route as for pure polyaniline. Modification comprised of adding powdered CaTi$_{0.8}$Fe$_{0.2}$O$_3$ to acetic acid (the mixture was sonicated for 30 min prior to addition) into the aniline solution. All of the following steps were the same as for pure polyaniline. In this way PANI-CaTi$_{0.8}$Fe$_{0.2}$O$_3$ nanocomposites were synthesized. The product was washed with water several times in order to remove unfused CTFO and then dried in an oven at 60°C for 24 h. In order to determine the amount of CTFO embedded in the PANI matrix, the composite samples were calcinated until a constant weight was achieved. The amount of CaTi$_{0.8}$Fe$_{0.2}$O$_3$ in the PANI-CTFO composite was 32 wt.% (PANI-32).

CHARACTERIZATION

[-] The morphologies of the products were examined by a scanning electron microscope (NOVA NANO SEM 200, FEI) equipped with an EDS analyzer (EDAX).

[-] The phase compositions and lattice parameters of the obtained sample discs (30 x 2 mm) were identified by X-ray diffraction analysis, based on the ICDD and ICSD databases. XRD measurements were taken using an Empyrean system (Panalytical) with monochromatic Cu K$_{\alpha1}$ radiation. The Rietveld refinement method was used for calculating the quantitative phase content and lattice parameters of the respective phases.

[-] Fourier transform infrared (FTIR) spectra of CaTi$_{0.8}$Fe$_{0.2}$O$_3$, PANI and PANI-CTFO were carried out on a mid-FTIR spectrometer Digilab Excalibur FTS 3000 Mx with an electrically cooled DTGS detector.

All the samples were pressed into a cylindrical dye to obtain clean discs of approximately 1 mm in thickness with a spectroscopic-grade KBr. Transmission spectra of the investigated samples were recorded in the range of 4000–400 cm^{-1}, at the resolution of 4 cm^{-1}. The number of scans was 128. Correction of the obtained spectra base line was performed by means of OMNIC 8 (Thermoscientific) software.

[-] For measuring the electrical conductivity of the samples, a measuring setup was implemented as shown in Figure 1. For the DC conductivity measurements, the setup consisted of a furnace powered by a temperature controller, sample holder with a construction allowing the measurement of 2-3 samples simultaneously in controlled atmosphere, with a gas supply system (MKS flow controllers) and data measurement-acquisition system (HP 34401 DMM, Kethley 2420 SMU and Keithley 7001 Switch system equipped with 7012 card). All the parts of the measuring system were computer controlled (measurement procedure prepared in Test-Point environment). For the ambient temperature humidity sensor measurements, the same sample holder was used, equipped additionally with a Delta OHM HD8901 Hygrometer to measure the relative humidity in the sample holder compartment. The samples were prepared as 10 mm discs with a 3 mm thickness by compacting appropriate powders in a pellet die using 0.5 MPa pressure. To ensure electric contact, a silver wire was bonded to the disc surface using silver paste.
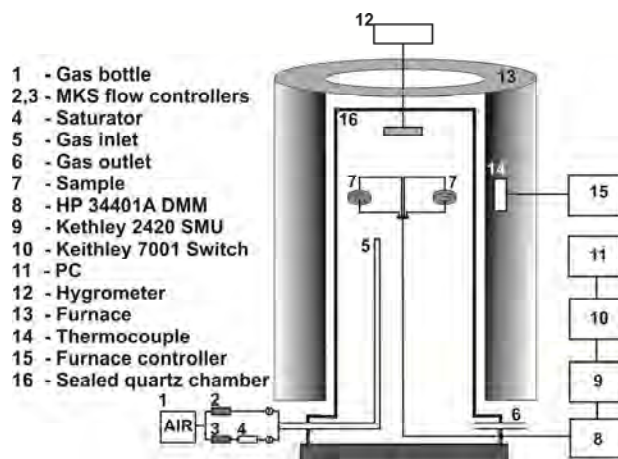

1   - Gas bottle
2,3 - MKS flow controllers
4   - Saturator
5   - Gas inlet
6   - Gas outlet
7   - Sample
8   - HP 34401A DMM
9   - Kethley 2420 SMU
10 - Keithley 7001 Switch
11 - PC
12 - Hygrometer
13 - Furnace
14 - Thermocouple
15 - Furnace controller
16 - Sealed quartz chamber

Fig. 1. Block scheme of humidity sensor set-up

Rys. 1. Schemat blokowy zestawu do pomiarów zmian przewodnictwa w funkcji wilgotności

RESULTS AND DISCUSSION

SEM study

The SEM micrograph of the CaTi$_{0.8}$Fe$_{0.2}$O$_3$ powder prepared by calcination at 600°C for 10 h is shown in Figure 2A. Most of the CTFO particles have irregular morphology, and the particle size is in the range 0.5÷3 μm. The addition of PEVA during the sol-gel process leads to the formation of cavernous structures in the CaTi$_{0.8}$Fe$_{0.2}$O$_3$ crystallites. An SEM micrograph

of polyaniline synthesized by the chemical oxidative method is shown in Figure 2B. Since acetic acid is used as protonic acid in the preparation of polyaniline, the presence of a semi-microcrystalline structure was observed. Moreover, it can be clearly seen that polyaniline forms a branched, sub-micron nanowire structure packed into bundles. The fibrous morphology of the microcrystalline structures was measured and found to be about 100 nm in diameter which is consistent with other reports [21].
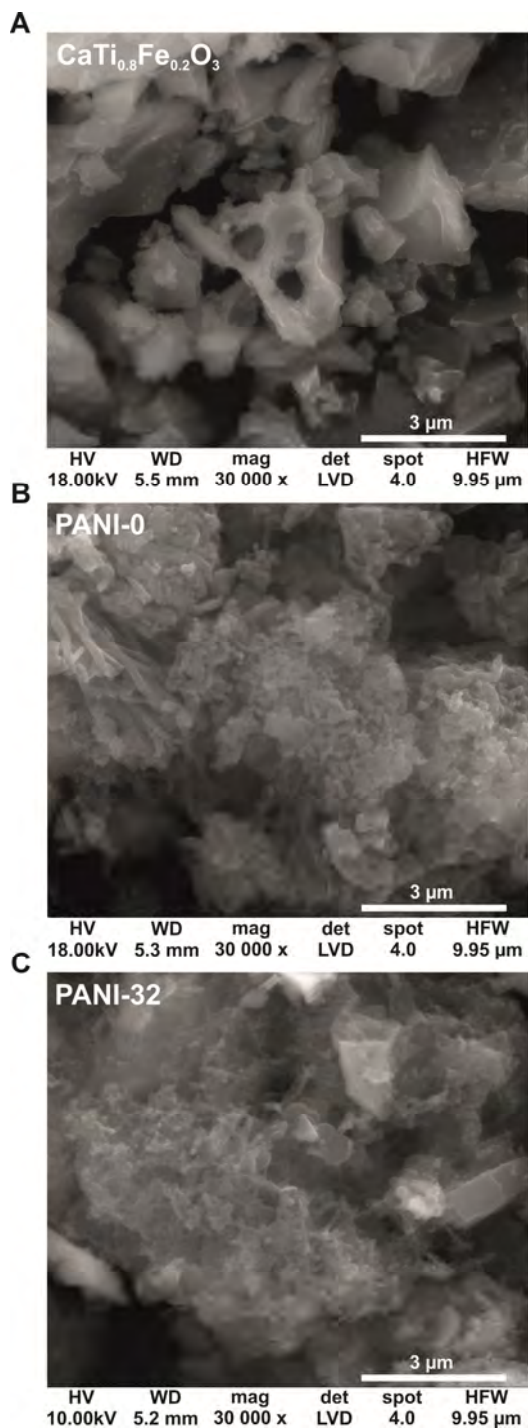

Fig. 2. SEM micrographs of (A) $CaTi_{0.8}Fe_{0.2}O_3$, (B) PANI and (C) PANI-32

Rys. 2. Mikrofotografie SEM przedstawiające strukturę próbek (A) $CaTi_{0.8}Fe_{0.2}O_3$, (B) PANI (C) PANI-32

The SEM image of PANI-$CaTi_{0.8}Fe_{0.2}O_3$ hybrid particles (shown in Figure 2C) reveals the presence of both composite components. It can be confirmed that the morphology of polyaniline does not differ from that of pure PANI. However, the fibers in the composite stack more tightly than the pure $CaTi_{0.8}Fe_{0.2}O_3$ nanoparticles. It can be noted that there are two kinds of particles in the composite. One is the free polyaniline particle, and the other is the composite particle that polyaniline encapsulates, $CaTi_{0.8}Fe_{0.2}O_3$. The composite particles are possibly glued or bound by the polyaniline chains.

FTIR study

The chemical structures of the products were confirmed by FTIR spectrum, and the results for $CaTi_{0.8}Fe_{0.2}O_3$, pure polyaniline, and the PANI-CTFO composite are displayed in Figure 3 respectively.
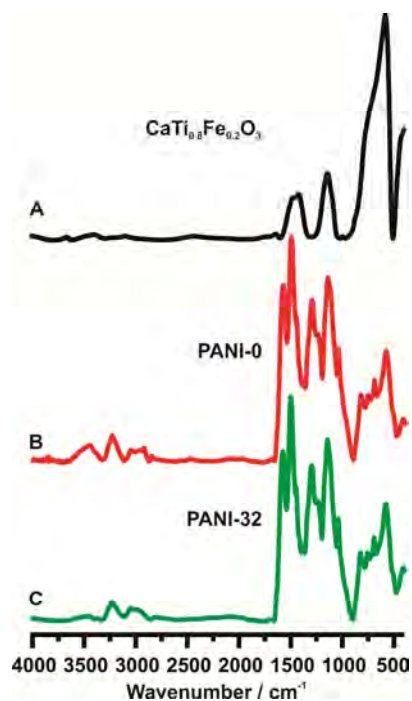

Fig. 3. FTIR spectra of (A) $CaTi_{0.8}Fe_{0.2}O_3$, (B) PANI and (C) PANI-32

Rys. 3. Widma FTIR przedstawiające (A) $CaTi_{0.8}Fe_{0.2}O_3$, (B) PANI (C) PANI-32

The FTIR spectrum of crystalline $CaTi_{0.8}Fe_{0.2}O_3$ obtained by the sol-gel method exhibits two large bands around 420 and 580 cm^{-1} that are caused by the stretching vibration due to the interactions produced between the oxygen and the metal bonds. The further appearance of two bands assigned to the deforming and stretching vibrations of hydroxylate - Ca-OH were observed at 1141 cm^{-1} for the former and 1436 cm^{-1} for the latter. The vibration of Ti-O-Fe was not observed, which may be ascribed to little substitution of Ti^{4+} by Fe^{3+} [22]. The FTIR spectra of PANI are somewhat altered to the most characteristic spectra of the granular form of polyaniline prepared in strong acidic conditions [23]. The fibrous texture of PANI has an impact on the molecular

structure of the polymer demonstrated by slight shifts in polymer chain vibrations. Nevertheless, the characteristic absorption bands of PANI are in accordance with those reported by the literature [24, 25] and are summarized in Table 1.

TABLE 1. **Characteristic FTIR bands of polyaniline**
TABELA 1. **Charakterystyka FTIR pasm polianiliny**

Band	Energy [cm^{-1}]	Vibration type
N-H	3450	stretching
N-H$_2$	1575	stretching
C=C (benzene ring)	1498	twisting
C-N (secondary imine)	1303	stretching
C-N (primary imine)	1241	stretching
C-H	1147	twisting
C-H (benzene ring)	825	stretching

The bands at 1041 and 583 cm^{-1} correspond to HSO$_4^-$ interacting with the N-H- group, since sulfuric acid is produced as a byproduct in the oxidation of aniline as shown in Figure 4 [26].
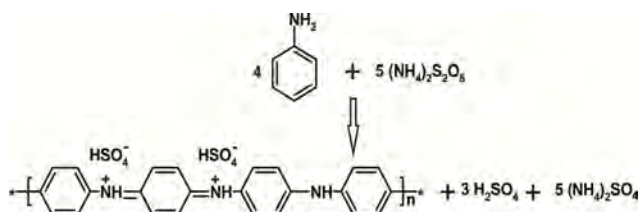

Fig. 4. Oxidation process of aniline by APS in acidic medium
Rys. 4. Reakcja polimeryzacji oksydacyjnej aniliny za pomocą APS w środowisku kwaśnym

In none of the samples was there a wide peak found in the region of 3400 cm^{-1}, which clearly shows the absence of moisture and molecular water bound to the mildly dry PANI. Nevertheless, both of the FTIR spectra of the pure polymer and PANI-32 samples reveal that the N-H stretching peak, which was observed as 3450 cm^{-1} in PANI-0, persists in the PANI-CTFO composite. This clearly indicates the occurrence of interaction between the H atoms in the N-H bond and the OH molecules. The appearance of this band was expected as the samples were not vacuum dried at elevated temperatures and some residual water still remained in the examined specimens. It should be noted that the spectra of PANI-32 does not exhibit any shifts due to substitution with CTFO, yet such behavior is observed for polymer composites doped with less than 50 wt.% inorganic oxide [27].

XRD study

The presence of diffraction peaks can be used to evaluate the long range order or periodicity of the material structure. The polycrystalline nature of the CaTi$_{0.8}$Fe$_{0.2}$O$_3$ powder is expressed by the XRD pattern

as shown in Figure 5A, which was identified as a tetragonal phase (I 4/m c m) with most the intense reflection peaks at 2θ values at 22.96°, 32.69°, 46.91°, 58.36°, and 68.51° corresponding to diffraction planes at (110), (112), (220), (132) and (224) respectively. All the peaks in the XRD pattern match well with the reported characteristic reflection peaks of CTFO - Card No. 98-005-1879 [28]. The observed X-ray diffraction pattern for the CaTi$_{0.8}$Fe$_{0.2}$O$_3$ particles shows a high degree of crystallinity. The crystallite size was estimated from the X-ray peak broadening of (h, k, l) diffraction using the Scherrer formula. The average grain size of the sample estimated from half the width of the XRD peak and found to be around 30 nm for CaTi$_{0.8}$Fe$_{0.2}$O$_3$. The XRD pattern of PANI arrayed in nanowires is illustrated in Figure 5B.
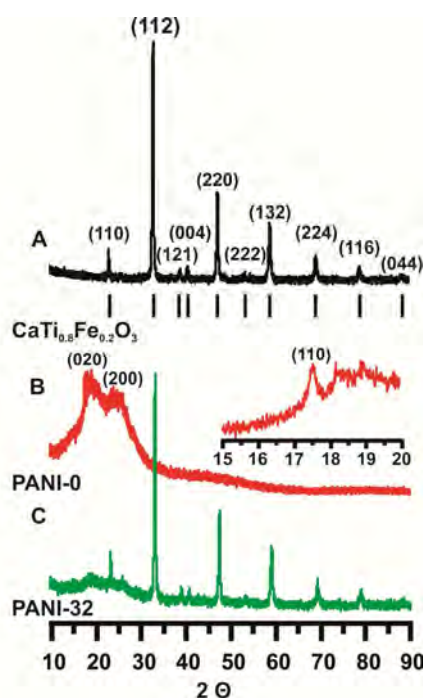

Fig. 5. XRD patterns of (A) CaTi$_{0.8}$Fe$_{0.2}$O$_3$, (B) PANI and (C) PANI-32
Rys. 5. Dyfraktogramy XRD przedstawiające próbki (A) CaTi$_{0.8}$Fe$_{0.2}$O$_3$, (B) PANI and (C) PANI-32

The amorphous nature of the sample is confirmed by the XRD spectrum, which shows broad peaks centered on 2θ ≈ 20.5° and 26.0°, which corresponds to the (020) and (200) diffraction planes related to a poorly crystallized polyaniline [29]. Thus the appearance of a sharp reflex at 17.5° demonstrates that the crystalline part of the PANI structure is significantly perturbed in such a sense that the preferential direction (011) is strongly privileged over (020) and (200), which corresponds to a polyaniline fibrous structure [30]. The X-ray diffraction pattern of PANI-32, a composite of polyaniline doped with 32 wt.% CaTi$_{0.8}$Fe$_{0.2}$O$_3$, is shown in Figure 5C. It is seen from this figure that the appearance the peaks of CTFO peaks indicates the crystalline nature of the composite. By associating the XRD patterns of the composite and CaTi$_{0.8}$Fe$_{0.2}$O$_3$, it is confirmed that

CTFO has retained its structure even though it is dispersed in PANI during the polymerization reaction [31].

DC conductivity

A variation of sample resistance as a function of temperature for PANI-0 and PANI-32 composite are presented in Figure 6A and 6B respectively. The comparison of the results obtained for PANI-0 and PANI-32 clearly indicates that the introduction of CTFO into the materials leads to a decrease in conductivity.
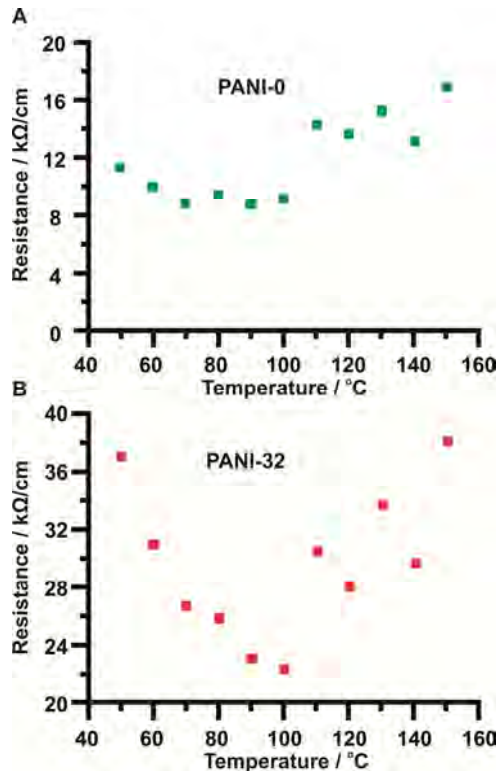

Fig. 6. (A) and (B) change in resistance against temperature of PANI-0 and PANI-32 respectively

Rys. 6. Zmiana oporności w funkcji temperatury dla próbek (A) PANI-0 oraz (B) PANI-32

The observed conductivity decrease cannot be explained only by the lower amount of conducting PANI phase, modification of the conducting mechanism (the partial blocking of the hopping of charge carriers) must be also taken into account. Two ranges of sample behavior can be noted in both samples. In temperatures between $50 \div 100^{\circ}$C, the conductivity values decrease, and rapidly increase in the temperature range of $100 \div 150^{\circ}$C. The temperature dependence in the temperature range $50 \div 100^{\circ}$C for both samples behaves in the usual activated manner indicating a semiconducting property. Literature suggests that electrical conduction in PANI is dominant by polarons and bipolarons that occur at the protonated polymer-vapor interface [32]. This would suggest that the conductivity increase with temperature is due to the increase in efficiency of the charge transfer making the water molecules favorable for electron

delocalization between the polymer and water molecules [33]. Above 100°C the amount of water decreases drastically leading to a decrease in PANI conductivity. Another aspect that should be taken into consideration is the thermal curing that effects the chain alignment of the polymer, which could lead to an increase in conjugation length combined with molecular rearrangement of the polymer chains on heating and would result in an increase in conductivity, although this effect does not compensate for the consequence of water evaporation [34].

In addition to resistance measurements, the current-voltage characteristics of PANI-0 and PANI-32 were performed as presented in Figures 7A and 7B respectively. Both samples exhibit resistor type behavior although pure polyaniline demonstrates nonlinear behavior whereas the polymer doped with $CaTi_{0.8}Fe_{0.2}O_3$ exhibits linear behavior in all the measured temperature ranges. It clearly indicates that the incorporation of dielectric CTFO (at low temperature) greatly modifies the electrical transport mechanism of the material, due to the presence of PANI-CTFO interfaces.
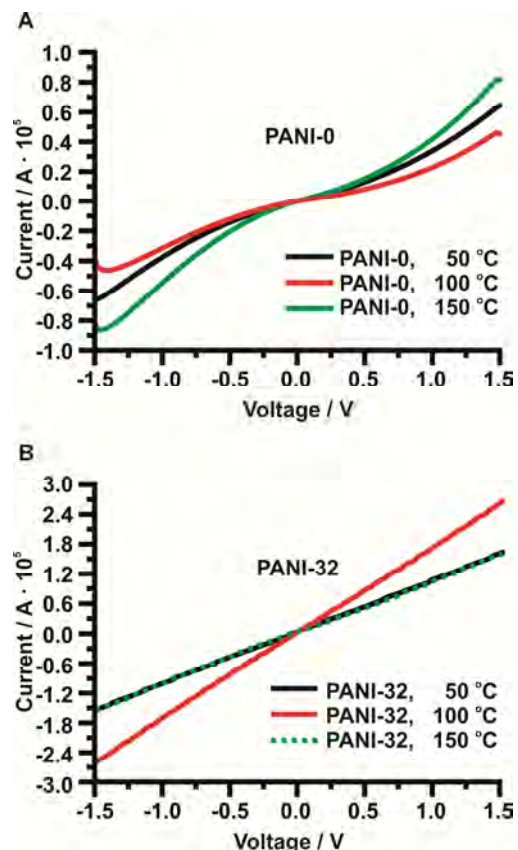

Fig. 7. (A) and (B) a current vs. voltage characteristics of PANI-0 and PANI-32 respectively

Rys. 7. Charakterystyki prądowo-napięciowe dla próbek (A) PANI-0 oraz (B) PANI-32

The observed influence of the CTFO phase on the electrical properties of PANI may be beneficial for applications where interphase phenomena are involved, e.g. for gas sensor constructions.

SENSING PROPERTIES

It was found that humidity would have a significant effect on the resistivity of PANI composite sensors [35]. Therefore, the effect of humidity on the performance of the PANI-32 sensor was investigated at ambient temperature, and the relationship between the resistance of the PANI and PANI-CTFO sensor and the relative humidity from 12 to 88% RH is shown in Figures 8A and B respectively. For both PANI-0 and PANI-32 the increase in the level of relative humidity [%] led to a reduction in sample resistivity.
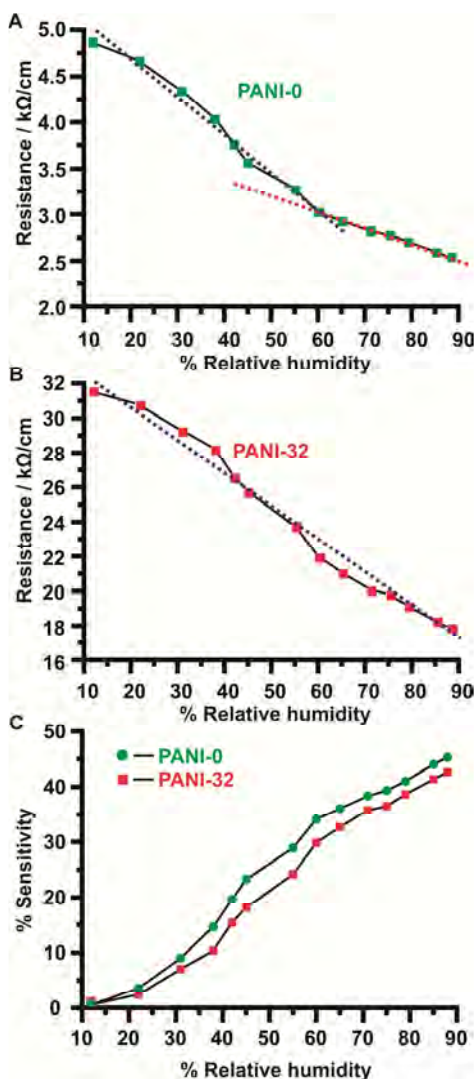

Fig. 8. (A) and (B) change in resistance against % RH of PANI-0 and PANI-32 respectively. Dashed lines mark trend lines in samples resistivity (C) sensitivity of PANI and PANI-32 as a function of % RH

Rys. 8. Zmiana oporności próbek w funkcji wilgotności względnej dla próbek (A) PANI-0 oraz (B) PANI-32. Linia przerywana obrazuje zmianę trendu w czułości próbek w miarę wzrostu wilgotności. (C) Graficzne porównanie czułości próbek PANI-0 oraz PANI-32 w funkcji wzrostu wilgotności względnej

The sensitivity of detecting humidity was defined by the percentage change in resistance as a function of relative humidity (RH). The percentage of sensitivity for detecting humidity can be defined as (equation 1):

$$S = \frac{R_{RH_1} - R_{RH_2}}{R_{RH_1}} \cdot 100\% \qquad (1)$$

where is the resistivity of the sample at the lowest humidity and is the resistivity of the sample at a specified RH. The sensitivity as a function of humidity of both samples is presented in Figure 8C.

It can be seen that in both cases for PANI-0 and PANI-32, when RH increases, the total resistance value decreases. Although for PANI-0 two ranges can be observed, whereas for PANI-32 the change in resistance is almost linear. In order to clearly explain the phenomenon of such an electrical response, several factors affecting polyaniline resistance need to be taken into consideration. In general, the total change in PANI electrical response (R$_{TOT}$) is a superposition of three major factors. The electronic effects (R$_{EE}$) that are associated with partial electron transfer between the polymer chains and residual absorbed water molecules. The electronic hopping process (R$_{EHP}$) demonstrates the effect of the swelling process that leads to looser packing of the polymeric chains. Finally, dielectric changes in the medium enclosed in PANI bulk (R$_{ME}$) represent variations in the dielectric constant of the solvent due to changes in its ion mobility and stabilization.

$$R_{TOT} = R_{EE} + R_{EHP} + R_{ME} \qquad (2)$$

Literature data suggest that the existence of water (or even some organic vapors) does not affect the electronic properties of PANI itself, therefore this effect was neglected in our considerations [36, 37]. Consequently, both R$_{EHP}$ and R$_{ME}$ should perform a dominant role in polyaniline and its composite conductivity, when humidity increases.

In humid conditions, the electron is transferred from the protonated reduced form (-NH$_2^+$-) to the protonated oxidized form (-NH$^+$=). Therefore, the reaction by which the proton is transferred to the water can be proposed as presented in Figure 9 [38].
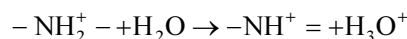
$$- NH_2^+ - + H_2O \rightarrow - NH^+ = + H_3O^+$$

Fig. 9. Simplified reaction scheme describing interaction between water molecules and polyaniline

Rys. 9. Uproszczony schemat reakcji obrazujący oddziaływanie pomiędzy cząsteczkami wody a polianiliną

Electron hopping assisted by proton exchange makes both PANI-0 and PANI-32 sensitive to water molecules as their conduction alters in the presence of H$_2$O molecules. Moreover the absorption of water vapor into the polymer matrix can work as a source of protons, which can either increase the doping level of the polymer or conduct a charge themselves through the network of absorbed water molecules [39]. The impact of both of those effects (R$_{EHP}$ and R$_{ME}$) can be seen in

the nonlinear reduction of PANI-0 resistance with increasing humidity. In the first zone up to about 60% RH, resistance decreases more rapidly at an increasing RH. It indicates that electrical conductivity increases as the pores, initially filled with dry air, are progressively filled with water which has a higher dielectric constant than air. In this zone the decrease in resistivity can be attributed mainly to the change in R_{ME}, because at a low % RH the polymer chains are densely packed in a compact coil form, whereas in high humidity conditions PANI with absorbed water molecules form a loose network that is more favorable for electron conduction [40]. Thus for a % RH range above 60 (second zone), the resistance decrease exhibits a milder slope. The absorption of H_2O particles into PANI bulk leads to expansion of the polymer matrix, hindering the electron hopping process [41]. Therefore it is worth noting that for PANI-32 an almost linear response is observed throughout the whole measured % RH range. This behavior can be attributed to the effect of CTFO doping as the polymer chain being fused to the perovskite grain probably exhibits a smaller tendency to separate in a humid environment, leading to better stability of PANI-32 at higher humidity levels. In addition to PANI-0 and PANI-32 sensing properties, resistance characterization of both samples was also performed. It should be noticed that both samples exhibit nonlinear resistance behaviour when low voltage is applied, as presented in Figure 10 A and B for PANI-0 and PANI-32 respectively.

Moreover, it ought to be pointed out that this effect is less manifested in the composite sample. Furthermore it is observed that for PANI-CTFO, an inversion of that effect at higher RH occurs. We can speculate that this inversion can be attributed to the PANI-CTFO-H_2O interface interactions, still further detailed research must be performed in order to directly understand this phenomenon.

CONCLUSIONS

We have successfully obtained $CaTi_{0.8}Fe_{0.2}O_3$ perovskite via the sol-gel method. Polyaniline-CTFO composites were obtained through the addition of iron doped calcium titanate to the polymerizing solution. Careful study of SEM micrographs revealed the fibrous nature of the polyaniline matrix, which is attributed to the usage of mild acidic conditions that appeared through initiation of the polymerization process. A further SEM study confirmed embedding of the perovskite powder in the PANI matrix. Characteristic polyaniline peaks were observed in the FT-IR spectra of both pure PANI and PANI-32. The XRD data confirmed that the synthesized $CaTi_{0.8}Fe_{0.2}O_3$ had a characteristic tetragonal perovskite structure, typical for this type of perovskite obtained at low calcination temperatures. Additionally, it was observed that the PANI-32 XRD patterns showed the presence of prominent peaks of a CTFO crystalline structure which indicates that perovskite has retained its structure in the composite form. DC conductivity shows that the conductivity increases with an increase in temperature until 100^oC due to the hopping protonated water molecules acting as charge carriers. Additionally, an addition of CTFO in PANI bulk exhibits a stabilizing effect on polyaniline resistor behavior. The variation of resistance as a function of % RH shows a decrease in resistance due to adsorption and absorption of water molecules on the surface of both polyaniline and the PANI-CTFO composite. Although PANI-32 sensing properties are marginally worse compared to PANI, still the composite exhibits a linear resistance decrease in a measured humidity range. Additionally both PANI and PANI-32 showed nonlinear resistance behavior when low voltage was applied, still this effect was less intense in the CTFO doped species. In general, an addition of iron doped calcium titanate into polyaniline bulk stabilizes the polymer structure at elevated temperatures. Moreover the PANI-CTFO composite shows comparable sensing properties and exhibits better linearity in the sensing response curve in all the measured humidity levels. Our work is still in progress to fully understand the inversion of resistance when low voltage is applied to the PANI-32 composite. This effect may be used to improve the constructed sensor performance, especially when low voltage is used.
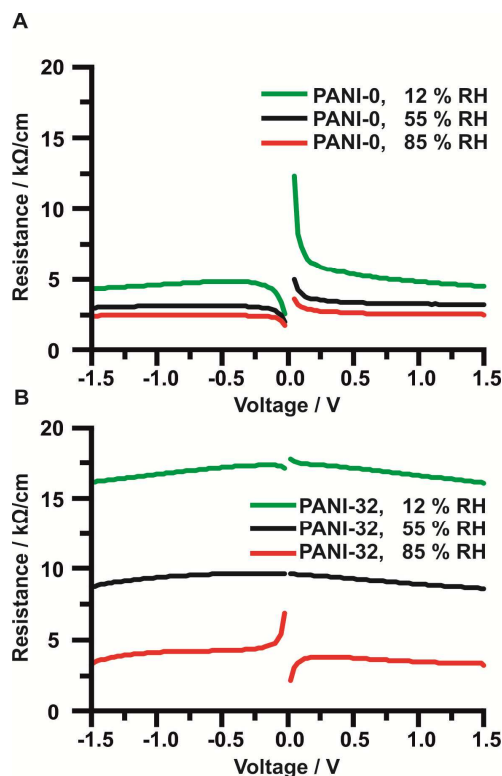

Fig. 10.   Resistance vs. voltage characteristics measured for PANI-0 and PANI-32 materials for different relative humidity

Rys. 10.   Zmiany w charakterystykach prąd-napięcie w wyniku zwiększania wilgotności względnej dla próbek (A) PANI-0 oraz (B) PANI-32

REFERENCES

[1] Chen Z., Lu C., Humidity sensors: A review of materials and mechanisms, Sens. Lett. 2015, 3, 274–295.

[2] Pawar S.G., Chougule M.A., Patil S.L., Raut B.T., Godse P.R., Sen S., Patil V.B., New method for fabrication of CSA doped PANI-TiO$_2$ sensor, IEEE Sen. J. 2011, 11, 3417-3423.

[3] Arshak E.M.K., Lyons G.M., Harris J., Clifford S., A review of gas sensors employed in electronic nose applications, Sens. Rev. 2004, 24, 181-198.

[4] Stejskal J., Sapurina I., Trchova M., Polyaniline nanostructures and the role of aniline oligomers in their formation, Prog. Poly. Sci. 2010, 35, 1420-1481.

[5] Letheby H., On the production of a blue substance by the electrolysis of sulphate of aniline, J. Chem. Soc. 1862, 15, 161-163.

[6] Genes E.M., Boyle A., Lapkowski M., Tsintavis C., Polyaniline: A historical survey, Synth. Met. 1990, 36, 139-182.

[7] Diaz A.F., Logan J.A., Electroactive polyaniline films, J. Electroanal. Chem. Inter. Electrochem. 1980, 11, 111-114.

[8] Sapurina I., Stejskal J., The mechanism of the oxidative polymerization of aniline and the formation of supramolecular polyaniline structures, Polym. Int. 2008, 57, 1295-1325.

[9] Łańcucki, Ł., Kruczała, K. Development of stabilized proton conducting membrane based on poly(ethylene-co-vinyl alcohol), Polym. Deg. Stab. 2014, 109, 327-335.

[10] Sonoda K., Juuti J., Moriya Y., Jantunen H., Modification of the dielectric properties of 0-3 ceramic-polymer composites by introducing surface active agents onto the ceramic filler surface, Compos. Struct. 2010, 92, 1052-1058.

[11] Kobayashi Y., Kurosawa A., Nagao D., Konno M., Fabrication of barium titanate nanoparticles-polymethylmethacrylate composite films and their dielectric properties, Polym. Eng. Sci. 2009, 49, 1069-1075.

[12] Windlass H., Raj P.M., Balaraman D., Bhattacharya S.K., Tummala R.R., Colloidal processing of polymer ceramic nanocomposites for integral capacitors, IEEE T. Electron. Pa. M. 2003, 26, 100-105.

[13] Chatterjee K., Dhara P., Ganguly S., Kargupta K., Banerjee D., Morphology dependent ammonia sensing with 5 - sulfosalicylic acid doped nanostructured polyaniline synthesized by several routes, Sensor. Actuator. B: Chem. 2013, 181, 544-550.

[14] Khuspe G.D., Navale S.T., Chougule M.A., Patil V.B., Ammonia gas sensing properties of CSA doped PANI-SnO$_2$ nanohybrid, Synth. Met. 2013, 185, 1-8.

[15] Talwar V., Singh O., Singh R.C., ZnO assisted polyaniline nanofibers and its application as ammonia gas sensor, Sensor. Actuator. B: Chem. 2014, 191, 276-282.

[16] Traversa E., Ceramic sensors for humidity detection: the state-of-the art and future developments, Sensor. Actuator. B: Chem. 1995, 23, 135-156.

[17] Wu L., Wu C.C., Wu M.M., Humidity sensitivity of Sr (Sn, Ti)O$_3$ ceramics, Journal of Electronic Materials 1990, 19, 197-200.

[18] Dunyushkina L.A., Electrophysical properties of titanates of alkaline-earth metals, Russ. J. Electrochem. 2007, 43, 894-900.

[19] Gorelov V.P., Balakireva V.B., Electroconductivity and nature of ionic transport in the calcium titanate-based substituted perovskites in humid atmosphere, Russi. J. Electrochem. 1997, 33, 1346-1350.

[20] Parveen A., Koppalkar A.R., Roy A.S., Surface modified CaTiO$_3$ loaded in polyaniline by sodium dodecyl benzene sulphonic acid for humidity sensor, IEEE Sensor J. 2012, 12, 2817-2823.

[21] Ciric-Marjanovic G., Blinova N.V., Trchova M., Stejskal J., Chemical oxidative polymerization of safranines, J. Phys. Chem B. 2007, 111, 2188-99.

[22] Yang H., Han C., Xue X., Photocatalytic activity of Fe-doped CaTiO$_3$ under UV-visible light, J. Env. Sci. 2014, 26, 1489-1495.

[23] Stejskal J., Sapurina I., Polyaniline: thin films and colloidal dispersions, Pure. Appl. Chem. 2005, 77, 815-26.

[24] Trchová M., Stejska J., Polyaniline, The infrared spectroscopy of conducting polymer nanotubes (IUPAC Technical Report), Pure. Appl. Chem. 2011, 83, 1803-1817.

[25] Xie S.H., Zhu B.K., Wei X.Z., Xu Z.K., Xu Y.Y., Polyimide/BaTiO$_3$ composites with controllable dielectric properties, Composite 2005, 36, 1152-1157.

[26] Stejskal J., Sapurina I., Trchova M., Polyaniline nanostructures and the role of aniline oligomers in their formation, Prog. Polym. Sci. 2010, 35, 1420-1481.

[27] Chen Q., Hong R.Y., Fabrication and characterization of Ba$_{0.5}$Sr$_{0.5}$TiO$_3$-PANI/PS three-phase composites, Ceram. Int. 2015, 41, 2533-2542.

[28] Seifert F., Knight K.S., Carpenter M.A., Redfern, S.A.T., Becerro A.I., Displacive phase transitions in and strain analysis of Fe-doped CaTiO$_3$ perovskites at high temperatures by neutron diffraction, J. Solid. State. Chem. 2002, 167, 459-471.

[29] Zhao G.Y., Li H.L., Preparation of polyaniline nanowire arrayed electrodes for electrochemical supercapacitors, Micropor. Mesopor. Mat. 2008, 110, 590-594.

[30] Abdolahi A., Hamzah E., Ibrahim Z., Hashim S., Synthesis of uniform polyaniline nanofibers through interfacial polymerization, Material. 2012, 5, 1487-1494.

[31] Parveen A., Koppalkar R.A., Ekhelikar S., Prasad M.V.N. A., Synthesis, characterization and electrical properties of polyaniline/SrTiO$_3$ composites, Mat. Sci. Res. Ind. 2009, 6, 179-183.

[32] Abdulla H.S., Abbo A.I. Optical and electrical properties of thin films of polyaniline and polypyrrole, Int. J. Electrochem. Sci. 2012, 7, 10666-10678.

[33] Chougule M.A., Pawar S.G., Godse P.R., Mulik R.N., Sen S., Patil V.B., Synthesis and characterization of polypyrrole (PPy) thin films, Soft Nanosci. Lett. 2011, 1, 6-10.

[34] Kobayashi A., Ishikawa H., Amano K., Satoh M., Hasegawa E., Electrical conductivity of annealed polyaniline, J. App. Phys. 1993, 74, 296-299.

[35] Sadek A.Z., Wlodarski W., Shin K., Bkaner R., Kalantar-Zadeh K., A layered surface acoustic wave gas sensor based on a polyaniline/In$_2$O$_3$ nanofibre composite, Nanotechnology 2006, 17, 4488-4492.

[36] Huang W.S., Mac Diarmid A.G., Optical properties of polyaniline, Polymer 1993, 34, 1833-1845.

[37] Kang E.T., Neoh K.G., Tan K.L., Polyaniline: A polymer with many interesting intrinsic redox states, Prog. Polym. Sci. 1998, 23, 277-324.

[38] Chani M.T.S., Karimov Kh. S., Khalid F.A., Moiz S.A., Polyaniline based impedance humidity sensors, Solid State Sci. 2013, 18, 78-82.

[39] Zeng F.W., Liu, X.X., Diamond D., Lau K.T., Humidity sensors based on polyaniline nanofibres, Sensor. Actuator B: Chem. 2010, 143, 530-534.

[40] Cavalloa P., Acevedoa D.F. Fuertesb M.C., Galo Soler-Illiab J.A.A., Barberoa C.A., Understanding the sensing mechanism of polyaniline resistive sensors. Effect of hu-midity on sensing of organic volatiles, Sensor. Actuator. B Chem. 2015, 210, 574-580.

[41] Roy A.S., Anilkumar K.R., Prasad M.V.N.A., Studies of AC conductivity and dielectric relaxation behavior of CdO--doped nanometric polyaniline, J. Appl. Polym. Sci. 2012, 123, 1928-1934.